# ICRF Mode Conversion Flow Drive on Alcator C-Mod

Y. Lin, J.E. Rice, S.J. Wukitch, M.L. Reinke, M.J. Greenwald, A.E. Hubbard, E.S. Marmar, Y. Podpaly, M. Porkolab, N. Tsujii, and the Alcator C-Mod team

Plasma Science and Fusion Center, Massachusetts Institute of Technology, Cambridge, MA, 02139, USA

e-mail contact of main author: ylin@psfc.mit.edu

**Abstract** ICRF mode conversion flow drive (MCFD) may be a candidate for the external control of plasma rotation in large tokamaks like ITER. Recently, we have carried out a detailed study of MCFD on the Alcator C-Mod tokamak, including its dependence on plasma and RF parameters. These results shed some light on the underlying physics and can help to extrapolate the method to other fusion devices. The flow drive efficiency is found to depend strongly on the $^3$He concentration in D($^3$He) plasmas, a key parameter separating the minority heating and mode conversion regimes. This result further supports the key role of mode conversion. The flow drive efficiency is also strongly affected by plasma density (~ $1/n_e$), that is, a power and/or momentum per particle dependence. Unlike the intrinsic rotation in L-mode, no dependence has been found on plasma topology (upper-null vs. lower-null). At +90$^o$ antenna phase (waves in co-$I_p$ direction) and dipole phase (waves symmetrical in both directions), we find that $\Delta V$ in the co-$I_p$ direction is proportional to the RF power, and also increases with $I_p$ (opposite to the $1/I_p$ intrinsic rotation scaling in H-mode). The flow drive efficiency is also higher at lower antenna frequency. A maximum central $\Delta V$ ~110 km/s at 2.7 MW $P_{RF}$ in L-mode has been achieved. Results in H-mode follow the same parametric scaling. However, the observed $\Delta V$ in H-mode has been small because of the much higher density and the unfavorable $1/n_e$ scaling. An empirical scaling law for +90$^o$ phasing and 180$^o$ phasing has been obtained. On the other hand, the behavior at -90$^o$ antenna phase is more complicated. At low RF power, $\Delta V$ at -90$^o$ phase is similar to the other phases, but at high $I_p$ and high power, the flow drive effect appears to be saturated (and to decrease) vs. RF power. This observation indicates that possibly two mechanisms are involved in determining the total torque: one is RF power dependent, which generates a torque in the co-$I_p$ direction, and the other is wave momentum dependent, i.e., the torque changes direction vs. antenna phasing.

## 1. Introduction

Plasma rotation (flow) and velocity shear can be important in stabilizing micro- and macro-instabilities in tokamak plasmas. Plasma rotation has been shown to be beneficial for tokamak plasma performance. Experimentally, sheared flow has been shown to improve plasma confinement [1,2,3], and a large toroidal rotation can help stabilize MHD modes [4,5], but the issue of plasma rotation drive and control on ITER is far from being resolved. The study of plasma rotation is currently a very active research field [e.g., 6,7,8,9,10,11]. In present tokamaks, externally driven rotation is mainly from neutral beam injection as a by-product of beam heating with direct angular momentum input to the plasma. However, for ITER, the neutral beam energy will be significantly higher in order to penetrate the expected higher density plasma and larger machine size, and this requirement will result in a much lower torque per MW beam power. Beam driven rotation is thus presumed to be small in ITER. Intrinsic rotation has been observed on many tokamaks [6, 7, 11,12], and it exists independent of the external momentum input or auxiliary heating method. For ITER and future reactors, active intrinsic rotation control will be difficult due to its correlation to plasma pressure and lack of profile control. Many efforts have been made on present tokamaks in search of an efficient RF flow drive method that may also be applicable on ITER and beyond. Experimentally, ICRF minority heated plasmas show no evidence of direct RF driven rotation. The rotation in ICRF minority heated plasmas on Alcator C-Mod has the same trend vs. plasma stored energy as the rotation in Ohmic plasmas [13,14]. Results from JET

[15,16,17], Tore-Supra [18,19] and ASDEX-Upgrade [20] all show that the contribution of ICRF minority heating to rotation is intrinsic, i.e., not directly from the RF power absorption but rather indirectly due to the change in the plasma temperature or plasma pressure.

ICRF mode conversion flow drive has been observed on Alcator C-Mod [21,22,23,24] and recently on JET [25,26,27]. In the previous Alcator C-Mod studies, we showed that ICRF mode conversion in D($^3$He) L-mode plasmas can drive significantly higher rotation than that from the empirical intrinsic rotation scaling. In this paper, we present results from a further study of the mode conversion flow drive method. We have studied the parametric dependence of the driven flow on a number of plasma parameters, including D(H) vs. D($^3$He), $^3$He concentration in D($^3$He) plasmas, B field, plasma current, plasma density, plasma shape, and in L-mode and H-mode, and also dependence on RF parameters like RF power, frequency and antenna phasing. An empirical scaling law has been obtained based on the parametric study.

## 2. Experimental setup and main diagnostics

Alcator C-Mod is a compact high field tokamak (R = 0.67 m, a = 0.22 m, and $B_{t0} \leq 8.1$ T). In this study, we ran plasmas with toroidal field as high as 8 T and plasma current up to 1.35 MA. There are two sets of ICRF antennas on Alcator C-Mod, and each of them is capable of coupling ~3 MW power to the plasma [28]. One system is phase variable (+90$^o$, -90$^o$, or 180$^o$), and also frequency tuneable (50, 70, or 78 MHz). The other system runs at a fixed frequency 80 MHz and fixed 180$^o$ phasing. At +90$^o$ phasing, the launched RF wave is preferentially in the same direction as the plasma current (co-$I_p$), while -90$^o$ phasing is counter-$I_p$ and 180$^o$ phasing (dipole) is toroidally symmetric.

We measure the plasma rotation by observing the Doppler shift of the H-like and He-like argon line emissions in the wavelength range of 3.7-4.0 Å. The spectra are obtained from a spatially resolving high resolution x-ray crystal spectrometer [29]. The instrument utilizes a spherically bent quartz crystal and a set of 2-dimensional x-ray detectors to image the entire plasma cross section with a spatial resolution about 1 cm and frame rate up to 200 Hz. In Fig. 1, we show an L-mode plasma ($B_{t0}$ = 8.0 T, $I_p$ = 1.2 MA, upper-single-null shape) with stepped-up ICRF power to 5 MW (78 MHz and 80 MHz). The central rotation velocity from the x-ray spectroscopy shown in Fig. 1-(a) increases up to ~100 km/s following the RF power steps. Positive velocity corresponds to rotation in the co-$I_p$ direction. This observation is independently corroborated by the measurement of n = 1 magnetic perturbations associated with sawtooth oscillations. The magnetic mode propagating velocity has been shown to be close to the plasma ion rotation velocity near q = 1 surface

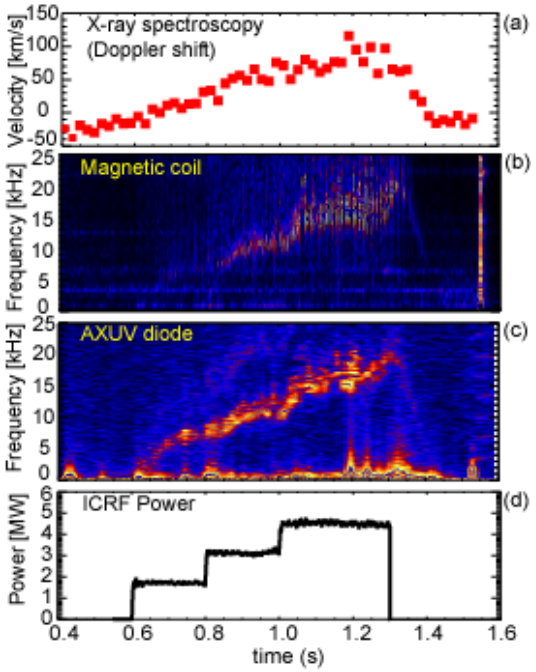


*FIG. 1. (a) Central toroidal velocity from X-ray spectroscopy; (b) and (c): frequencies of magnetic perturbation from a magnetic coil and an AXUV diode; (d) RF power trace (78 and 80 MHz). $B_{t0}$ = 8.0 T, $I_p$ = 1.2 MA, $n_{e0} = 1.6\times10^{20}$ $m^{-3}$.*

(R ~ 0.75 m for this plasma) [14 ]. Therefore, the mode frequency up to 20 kHz shown in Fig. 1-(b) and 1-(c) corresponds to a plasma rotation velocity of $2\pi R \times f \sim 95$ km/s, similar to the x-ray spectroscopy measurement.

The mode converted waves are detected by a phase contrast imaging (PCI) system [30,31]. The wave detection can help us estimate the concentration of the $^3$He level, and also help benchmark the simulation codes.

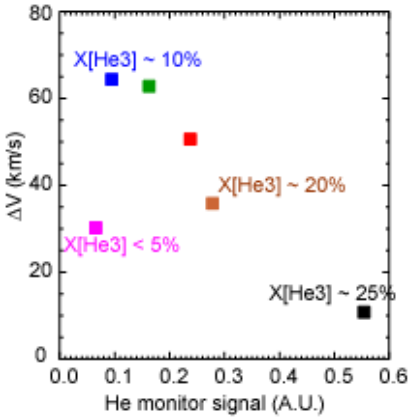


*FIG. 2. The change of central rotation velocity vs. $^3$He monitor signal. The concentrations are estimated from PCI measurement.*

## 3. Mode conversion heating vs. minority heating

In D($^3$He) plasmas, the concentration of $^3$He, X[$^3$He] = $n_{He3}/n_e$, determines whether the fast wave launched by the antenna is heating via minority heating (MH) or mode conversion (MC) heating. A larger X[$^3$He] also moves the mode conversion (MC) layer further away from the ion cyclotron (IC) layer in the direction toward the high field side. The distance between MC layer and IC layer also strongly affects how the RF wave power is deposited. In Fig. 2, the central velocities of a series of plasmas are plotted vs. $^3$He monitor signal. All the plasmas have $I_p$ = 0.8 MA, $B_t$ = 5.1 T, $n_{e0} = 2.0\times10^{20}$ m$^{-3}$, and $P_{RF}$ = 2.5 MW at 50 MHz and at +90$^o$ phasing. X[$^3$He] is inferred from the location of the MC waves measured by PCI. Fig. 2 shows that the rotation maximizes at X[$^3$He] ~ 10%, and at both low and high levels of X[$^3$He], the rotation velocities are smaller. This result suggests that an intermediate level of $^3$He is conducive for flow drive.

We have also compared the rotation from the typical D($^3$He) flow drive scenario with the routinely used D(H) minority heating scenario on C-Mod. In Fig. 3-(a), we compare two L-mode upper-single-null plasmas that have the same $B_t$, $I_p$, and $n_e$, but one is heated with D($^3$He) mode conversion at 50 MHz and the other one heated with D(H) minority scenario at 80 MHz. In this setup, the H IC layer in the D(H) plasma is at the same position as the $^3$He IC layer in the D($^3$He) plasma. At the same RF power the D($^3$He) MC heated plasma shows a much larger change of rotation. Two different RF frequencies were used in this comparison, and as discussed later in this paper, RF frequency can affect the flow drive efficiency. In Fig. 3-(b), we compare two plasmas with

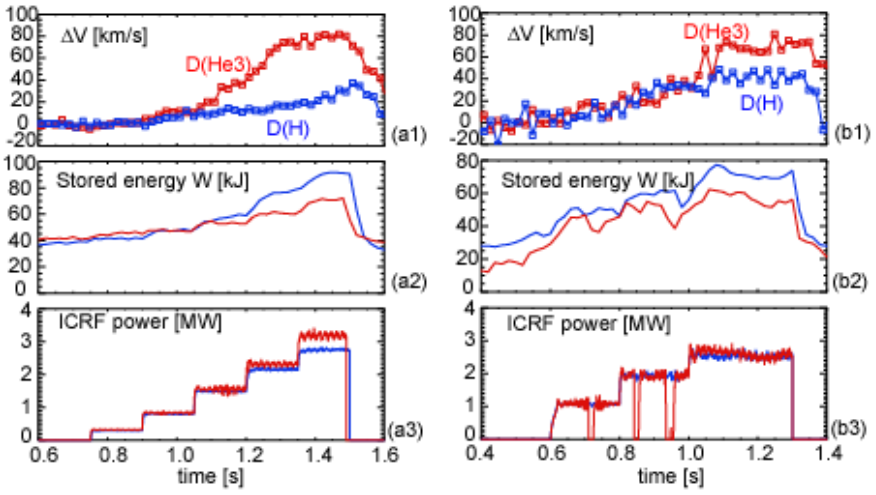


*FIG. 3. Central rotation velocity, stored energy and ICRF traces. (a)-a3): $B_{t0}$ = 5.1 T, 1.0 MA, $n_{e0} = 1.5\times10^{20}$ m$^{-3}$,50 MHz for D($^3$He) and 80 MHz for D(H); (b1-b3): 70 MHz, 1.0 MA, $n_{e0} = 1.6\times10^{20}$ m$^{-3}$, $B_{t0}$ = 4.6 T for D(H) and 7.2 T for D($^3$He).*

D($^3$He) MC and D(H) MH at the same RF frequency 70 MHz, but at different B fields to have the same IC layer position. Again, the plasma at D($^3$He) mode conversion shows a much larger rotation change. The rotation velocity in the MH plasmas follows the well-established empirical $\Delta W/I_p$ scaling [13] (where W is the plasma stored energy). The velocity change $\Delta V_\phi$ of the MC plasmas is approximately linear vs. the level of the applied RF power. For the cases shown in Fig. 3, the MC flow is larger than that from the intrinsic rotation (even at smaller change in plasma stored energy).

### 3. Dependence on antenna phasing, RF power and plasma current

At 180$^o$ (dipole) phasing, the net ICRF wave momentum is approximately zero, while at +90$^o$ and -90$^o$ phasings, the fast waves carry momentum. In our experiment, we have studied the effect of the antenna phasings. In Fig. 4, we show the frequency of the magnetic perturbation and rotation velocity from X-ray spectroscopy of two discharges with different antenna phasings, but identical plasma parameters ($I_p$ = 1.2 MA, $B_{t0}$ = 7.9 T, $n_{e0}$ = $1.9\times10^{20}$ m$^{-3}$, and $P_{RF}$ = 2.5 MW at 78 MHz). The plasma with +90$^o$ phasing has larger rotation than that from -90$^o$ phasing. This result suggests that the antenna phasing can affect the rotation in the MC flow drive.

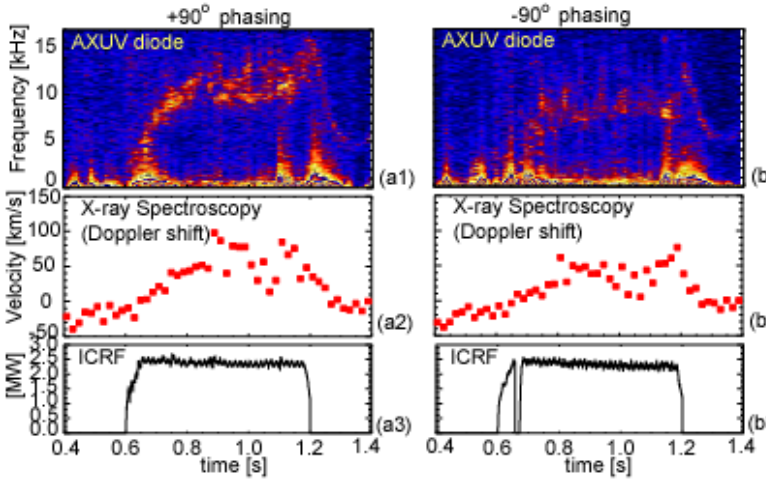


*FIG. 4. Magnetic perturbation frequency, central rotation velocity and RF power traces. (a1-a3): +90$^o$ phasing; (b1-b3): -90$^o$ phasing. $I_p$ = 1.2 MA, $B_{t0}$ = 7.9 T, $n_{e0}$ = $1.9\times10^{20}$ m$^{-3}$, ICRF frequency 78 MHz.*

Further experiments show that the effect of the antenna phasing is complicated, and it depends on $I_p$ and $P_{RF}$. In Fig. 5, we show the traces of comparable plasmas at different antenna phasings. In Fig. 5-(a), the plasmas are all with $I_p$ = 1.2 MA. We note that the rotation velocities at all three phasings are similar for $P_{RF}$ < 2 MW, while at the higher RF power, the flow drive effect diverges: Increasing ICRF power at +90$^o$ phasing drives larger co-$I_p$ rotation, and the rotation from dipole phasing also increases albeit at a slower rate, while at -90$^o$ phasing, the rotation actually decreases. A

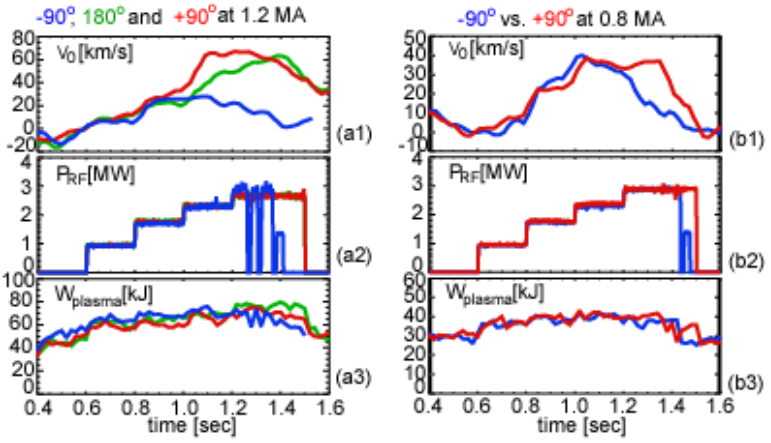


*FIG. 5. Central rotation velocity, RF power, and stored energy trace vs. antenna phases and $I_p$. (a1-a3)$I_p$ = 1.2 MA; (b1-b3) $I_p$ = 0.8 MA. $B_{t0}$ = 5.1 T and ICRF frequency 50 MH, $n_{e0}$ = $2.0\times10^{20}$ m$^{-3}$.*

similar conclusion can be made from Fig. 5-(b) where the flow drive effect diverges at $P_{RF}$ > 2.3 MW for $I_p$ = 0.8 MA.

In Fig. 6, we plot the scaling of the central rotation velocity vs. $P_{RF}$ at different $I_p$ for +90° phasing and -90° phasing. For +90° phasing (Fig. 6-(a)), an approximately linear scaling of ΔV vs. $P_{RF}$ holds for all plasma currents. For the same $P_{RF}$, ΔV is also generally larger at larger plasma current. In contrast, for -90° phasing (Fig. 6-(b)), the RF power level beyond 2 MW does not drive more co-$I_p$ rotation. The rotation saturation level does not seem to depend on the plasma current. This observation suggests that the direct RF momentum input does affect the magnitude of the flow drive. It is also possible that another mechanism masks the flow drive effect at -90° phasing. For example, with RF heating, the intrinsic rotation would rise in the co-$I_p$ direction. The flow drive torque from the high power input at -90° phasing might have been strongly counter-$I_p$ if there were no effect from intrinsic rotation. Future experiments will be necessary to clarify this issue.

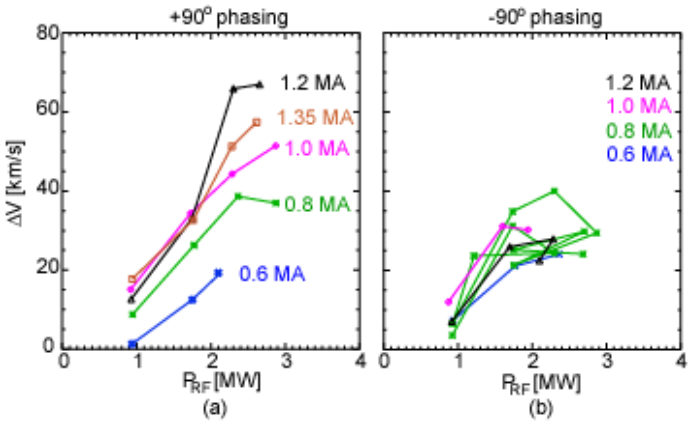


*FIG. 6. Central rotation velocity vs. RF power: (a) +90° phasing; (b) -90° phasing. $B_{t0}$ = 5.1 T, RF frequency 50 MHz, $n_{e0} = 1.9\times10^{20}m^{-3}$.*

## 4. Dependence on plasma density, shape, L and H-modes

In Fig. 7, we show the results from a shot by shot plasma density scan of the mode conversion flow drive. All the plasmas are in L-mode, and have $I_p$ = 1 MA, $B_t$ = 5.1 T, $P_{RF}$ = 2.5 MW at 50 MHz and at +90° phasing. The rotation velocities are as high as 100 km/s at low density and as low as 20 km/s at high density. Such strong dependence on density clearly shows that lower density is favoured for the flow drive. This density scan was carried out for the upper-single-null (USN) plasmas, where the power threshold for the L-mode to H-mode transition is much higher than the typical lower-single-null (LSN) plasmas. Unlike the intrinsic rotation, the flow drive effect in LSN plasmas is shown to be very similar to that in USN plasmas for power levels below the L-H transition power threshold, thus we can rule out that plasma shape plays a significant role. Launching RF power into H-mode plasmas does not drive significant rotation in addition to the rotation rising from the intrinsic rotation. This weak effect in H-mode is likely due to the much higher density that in L-mode, while stored energy is also higher for a given power. The obtained H-mode data points follow the same empirical scaling (see Section 6) as those from L-mode plasmas. Further study of flow drive in other high confinement modes without a density rise,

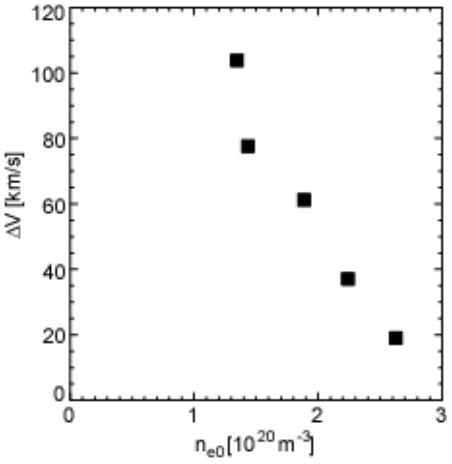


*FIG. 7. Central rotation velocity vs. plasma density. $P_{RF}$ = 2.6 MW @ 50 MHz, +90° phasing, $B_{t0}$ = 5.1 T, $I_p$ = 1* MA

for example, the so-called I-mode [32], will help us study whether possibly better momentum confinement can improve the flow drive efficiency.

## 5. Dependence on B field and RF frequency

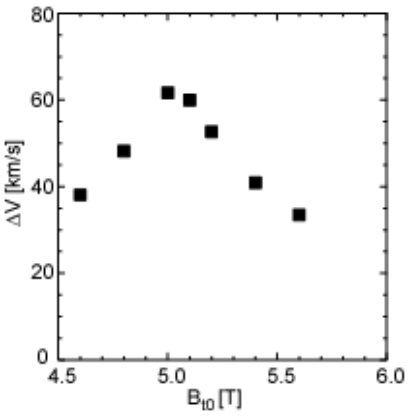


*FIG. 8. Rotation velocity vs. B field. $I_p$ = 0.8 MA, ICRF 2.6 MW @ 50 MHz, $n_{e0} = 1.8\times10^{20}m^{-3}$.*

Changing the toroidal B field at a constant RF frequency moves the location of the MC layer and IC layer and can also affect the flow drive efficiency. Fig. 8 shows the result of a series of identical plasmas ($I_p$ = 0.8 MA, $n_{e0}$ = $1.8\times10^{20}m^{-3}$) at different B fields while heated with $P_{RF}$ = 2.6 MW at 50 MHz and +90° phasing. The largest rotation is obtained for $B_{t0}$ ~ 5.0-5.1 T. At this field, the $^3$He cyclotron layer is a few cm on the low field side of the magnetic axis, and the mode conversion layer (D-$^3$He hybrid layer) is also a few cm on the high field side of the axis. Similar B field scans have been carried out at 70 MHz and 78 MHz, and in general, making both the MC layer and IC layers close to the plasma axis is found to drive the largest central toroidal rotation. However, the flow drive efficiency at different frequencies is different even at the respectively optimized $B_{t0}$. In Fig. 9, we show two plasmas having the same $I_p$ = 1 MA, $^3$He concentration, $n_{e0}$ = $1.4\times10^{20}m^{-3}$ and $P_{RF}$ = 2.5 MW at +90° phasing, but one is at 70 MHz/7.2 T and the other one at 50 MHz/5.1T. These two plasmas show very similar changes of plasma stored energy, but the change of rotation velocity in the 50 MHz plasma, ~80 km/s, is much larger than that from the 70 MHz plasma, ~55 km/s. The ratio of the velocities is approximately the inverse ratio of the frequencies (or equivalently, $B_{t0}$). Since the momentum carried by the RF waves is inversely proportional to the frequency for the same toroidal antenna structure, the dependence on RF frequency indicates the RF momentum input plays an important role in flow drive.

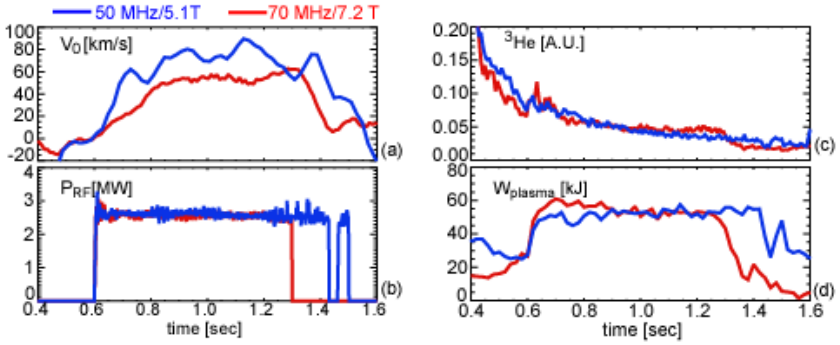


*FIG. 9. Central rotation velocity at two different antenna frequencies (blue:50 MHz and $B_{t0}$=5.1T; red: 70 MHz and $B_{t0}$ = 7.2 T). $I_p$ = 1 MA, +90° phasing, $n_{eo} = 1.4\times10^{20}m^{-3}$.*

## 6. Empirical scaling law of the flow drive efficiency

Our detailed experimental study has revealed the dependence of the flow drive efficiency vs. X[$^3$He], plasma current, plasma density, and RF power, frequency and antenna phasing. The result from -90° antenna phasing is complicated, but the flow drive efficiency at +90° and 180° appears to have clear parametric dependences. Using all the data from dedicated experiments, we have carried out a multiple-parameter regression and obtained an empirical scaling law for the +90° and 180° phasings (with X[$^3$He] ~ 10%). The resulted scaling law is: $\Delta V[km/s] \approx 7.5\times10^2 P_{RF}[MW]^{1.3} I_p[MA]^{0.5} n_{e0}[10^{20} m^{-3}]^{-0.9} f[MHZ]^{-0.8}$. Data from different

antenna frequencies and confinement modes are separately plotted in Fig. 10. Note the intrinsic rotation on Alcator C-Mod (Ohmic and minority heating plasmas) approximately follows $\Delta W/I_p$ scaling. In Fig. 11, we compare the mode conversion flow drive data to the intrinsic rotation scaling. Because with RF heating the stored energy generally rises, it is no surprise that a general trend vs. $\Delta W$ exists in the database. However, the data are much more scattered to be fit with this simple $\Delta W/I_p$ scaling. While the rotation velocities from 78 MHz are not significantly different than that from this intrinsic scaling, those from 50 MHz and 70 MHz are much larger (note that both axes of the graph are logarithmic).

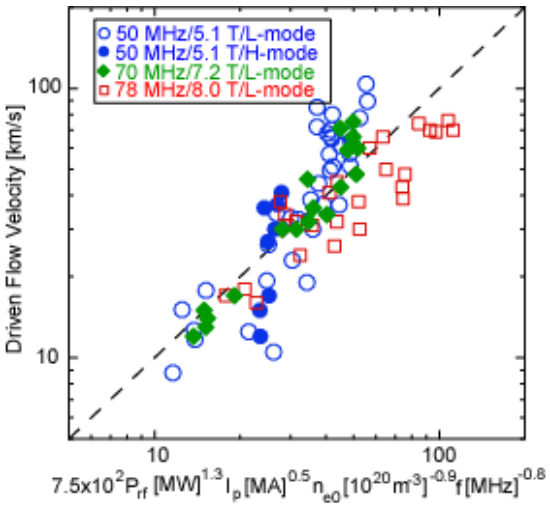


*FIG. 10. Empirical scaling law for all the data from 180$^o$ and +90$^o$ antenna phasing.*

The empirical scaling law of MC flow drive, approximately $P_{rf}\sqrt{I_p}/n_e f$ , indicates that the ICRF power (or momentum) per particle plays an important role. The positive dependence on $I_p$ may suggest a momentum confinement scaling (similar to energy scaling). In addition, $I_p$ can also affect the mode conversion to the ion cyclotron wave by varying the poloidal B field [30]. The interaction between the mode converted ion cyclotron waves and the $^3$He ions, and its associated momentum asymmetry has been thought to be the key to generate the flow [22,23,27]. The experimental observation for +90$^o$ phasing is consistent with this conjecture. But the complicated $P_{RF}$ and $I_p$ dependence for -90$^o$ antenna phasing indicates that possibly two mechanisms are involved in determining the total torque: one is RF power dependent, which generates a torque in the co-$I_p$ direction, and the other is wave momentum dependent, i.e., the torque changes direction vs. antenna phase. Further experimental work and modelling will be required to identify the detailed mechanisms.

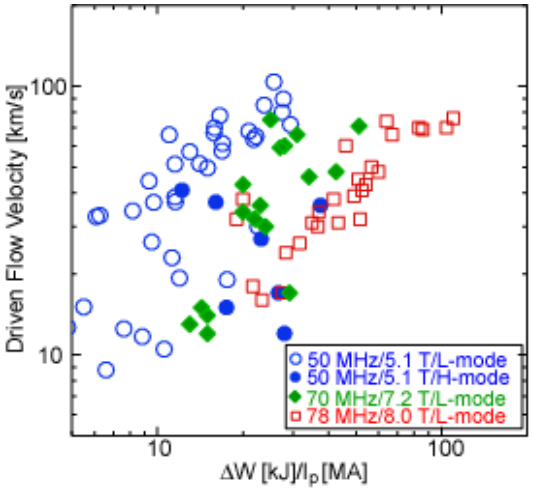


*FIG. 11. MCFD rotation velocity plotted against the intrinsic rotation scaling for all the data of 180$^o$ and +90$^o$ antenna phasing.*

## 7. Summary

ICRF mode conversion flow drive has been studied in detail on Alcator C-Mod. The flow drive efficiency has been shown to depend on the ICRF power, frequency, and antenna phasing, the level of $^3$He concentration in D($^3$He) plasmas, plasma density, plasma current, and B field. An empirical scaling law has been obtained for the +90$^o$ phasing and dipole phasing. At -90$^o$ phasing, the parametric dependence is more complicated, and in general, the co-$I_p$ rotation velocity is smaller. The experimental evidence suggests both the ICRF heating and momentum carried by the wave play roles in driving the flow.

**Acknowledgments**

The authors thank the Alcator C-Mod operation and ICRF groups. This work was supported at MIT by U.S. DoE Cooperative Agreement No. DE-FC02-99ER54512.

**References**

[1] Burrell K.H. 1997 *Phys. Plasmas* **4** 1499
[2] Politzer P.A. *et al* 2008 *Nucl. Fusion* **48** 075001
[3] Mantica P. *et al* 2009 *Phys. Rev. Lett.* **102** 175002
[4] Strait E.J. *et al* 1995 *Phys. Rev. Lett.* **74** 2483
[5] Garofalo A.M. *et al* 2001 *Nucl. Fusion* **41** 1171
[6] Rice J.E. *et al* 2007 *Nucl. Fusion* **47** 1618
[7] deGrassie J.S. *et al* 2009 *Plasma Phys. Control. Fusion* **51** 124047
[8] Tala T. *et al* 2009 *Phys. Rev. Lett.* **102** 075001
[9] Rice J. *et al* 2009 *Nucl. Fusion* **49** 025004
[10] Yoshida M. *et al* 2009 *Phys. Rev. Lett.* **103** 065003
[11] Solomon W. *et al* 2010 *Phys. Plasmas* **17** 056108
[12] Bortolon A. *et al* 2006 *Phys. Rev. Lett.* **97** 235003
[13] Rice J.E. *et al* 1999 *Nucl. Fusion* **39** 1175
[14] Hutchinson I.H. *et al* 2000 *Phys. Rev. Lett.* **84** 3330
[15] Eriksson L.-G., *et al* 1997 *Plasma Phys. Control. Fusion* **39** 27
[16] Eriksson L.-G., *et al* 2009 *Plasma Phys. Control. Fusion* **51** 044008
[17] Noterdaeme J. M., *et al* 2003 *Nucl. Fusion* **43** 274
[18] Assas S. *et al 30th EPS Conf. on Plasma Physics and Controlled Fusion* (St Petersburg, Russia, 7-11 July 2003) ECA **27A,** P-1
[19] Eriksson L.-G. *et al* 2001 *Nucl. Fusion* **41** 91
[20] Assas S. *et al* 2007 *Radio Frequency Power in Plasmas,* edited by P.M. Ryan and D. A. Rasmussen, *AIP Conference Proceedings* **978** 103
[21] Lin Y., *et al 22nd IAEA Fusion Energy Conference,* Geneva, Switzerland (2008) PD1- 2
[22] Lin Y., *et al* 2008 *Phys. Rev. Lett.* **101** 235002
[23] Lin Y., *et al* 2009 *Phys. Plasmas* **16** 056102
[24] Rice J.E., *et al 37th EPS conference on Plasma Physics* (Dublin, Ireland, 21-25 June, 2010).
[25] Tala T., *et al 23rd IAEA Fusion Energy Conference,* Daejeon, Korea (2010) EX3-1
[26] Lin Y., *et al 37th EPS Conf. on Plasma Physics and Controlled Fusion* (Dublin, Ireland, June 2010).
[27] Lin Y., *et al* "ICRF mode conversion flow drive in D($^3$He) plasmas on JET", *to be submitted to Plasma Phys. Control. Fusion*
[28] Bonoli P., *et al* 2007 *Fusion Sci. Tech.* **51** 401
[29] Ince-Cushman A. *et al* 2008 *Rev. Sci. Instrum*. **79** 10E302
[30] Nelson-Melby E. *et al* 2003 *Phys. Rev. Lett.* **90** 155004
[31] Lin Y. *et al* 2005 *Plasma Phys. Control. Fusion* **47** 1207
[32] Whyte D. *et al* 2010 *Nucl. Fusion* **50**, 105005.